

# New type of microengine using hydrogen and oxygen

This would have to be the worlds smallest combustion engine with the dimensions  $100 \times 100 \times 5 \mu\text{m}^3$  that is using internal combustion of hydrogen and oxygen as part of its working cycle. The following is an abstract form a recent paper on the topic.

I thought it was about time we got back to some real science. I am often distracted by free energy claims (and the lack of science that goes with it), It is like waving a reg flag to a bull, a weakness in my character I should work on. On with real science.

What is even more amazing about this development which also uses hydrogen and oxygen, is the scientists have some theories on how it works but are not entirely sure. The reason for developing this is electric motors and magnetic actuators do not scale down well. The scientists wanted something small with a big bang for the buck. In their own words “micro systems suffer from lack of strong and fast actuators. Small electromagnetic motors cannot generate forces of useful magnitude but internal combustion engines just do not exist at the micro scale.”

## Introdcution

Existing microactuators are using mostly two types of forces:

- a. electrostatic forces (weak)
- b. and those generated by thermal expansion (slow).

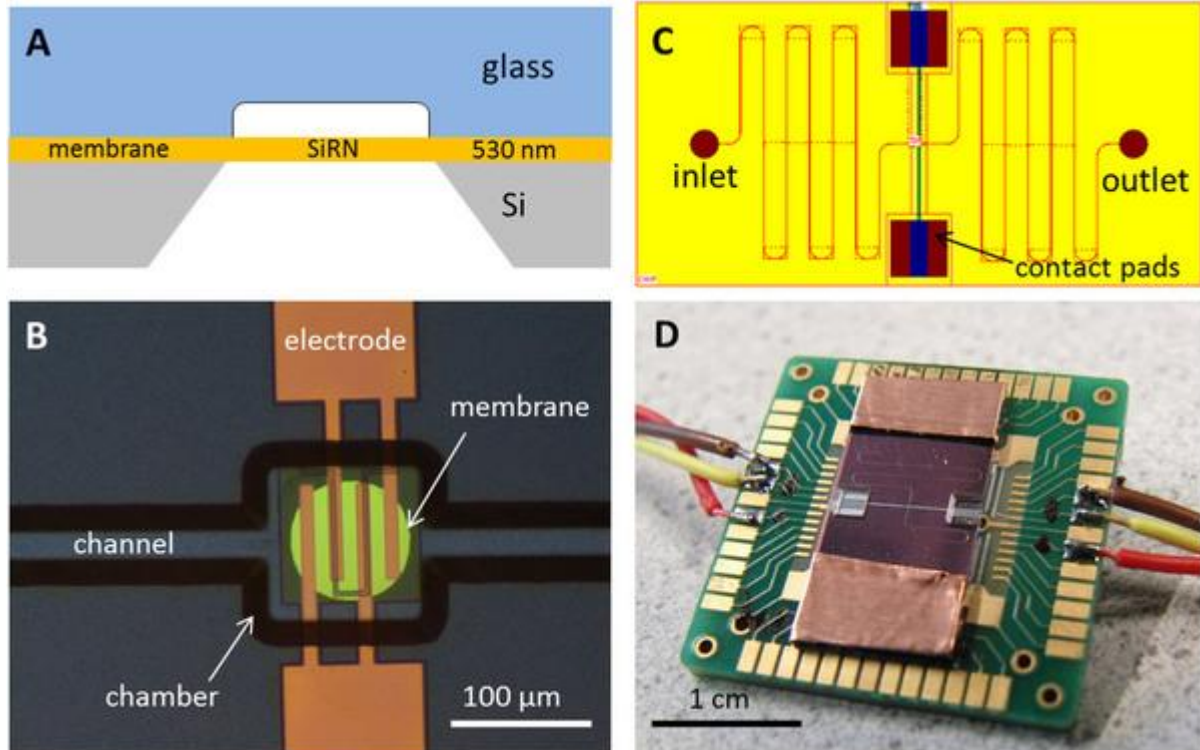
Small electromagnetic motors cannot generate forces of useful magnitude but fast and strong piezoelectric elements are not compatible with microtechnology and need a high voltage for actuation. Some progress was achieved with the use of electroactive polymers but they are not suitable for many applications in microsystems. Electrochemical actuation was also discussed in many papers but it is notoriously slow. One can produce a large amount of gas in a short time but it is impossible to get rid of this gas also fast. In this paper we present an actuator that uses **alternating polarity (AP) short-time electrolysis to produce H<sub>2</sub> and O<sub>2</sub> gases but termination of the gases happens very fast due to spontaneous combustion.**

**Microengines using gas combustion perform poorly** due to increased heat losses via the volume boundary when the volume decreases. However, recently we observed that the reaction between H<sub>2</sub> and O<sub>2</sub> gases can be ignited spontaneously in stoichiometric nanobubbles smaller than 200 nm overcoming this restriction in some way. The mechanism is still not clear, but it is expected that both high Laplace pressure and fast dynamics are important<sup>6</sup>. It is not obvious that the reaction in nanobubbles and performance of the microscopic actuator are related. Nevertheless, we speculate that the gas combustion in the chamber happens via combustion in transitional nanobubbles. Nanobubbles already demonstrated counterintuitive properties such as unexpectedly long life time of the surface nanobubbles. Mechanism of this stability is still debated after more than 10 years of active discussion.

### **Fabrication and characterization**

The actuators were fabricated on Si wafers covered with a layer of silicon rich nitride (SiRN) (thickness 530 nm) containing deposited Pt electrodes of different designs. This layer played the role of the actuator membrane. The membrane was made free by etching the wafer from the back side. The chamber and filling channels were isotropically etched in borofloat wafers. The glass and Si wafers were anodically bonded as shown in [Fig. 1](#). A polysilicon thermal sensor designed for four-probe measurements was fabricated underneath the electrodes (see details in [Supplementary](#)). The bonded wafers were diced into separate chips with the size  $2 \times 1 \text{ cm}^2$ . The actuator chamber with the nominal dimensions  $100 \times 100 \times 5 \text{ }\mu\text{m}^3$  was filled via the channel (cross section  $10 \times 5 \text{ }\mu\text{m}^2$ ) with a solution of Na<sub>2</sub>SO<sub>4</sub> in deionized water. In most cases the salt concentration was around 1 M. The inlet and outlet openings were sealed with a foil, the chip was glued to a printed circuit board (PCB) with an opening in the middle to get access to the membrane from the back side. For one chip without the covering glass we calibrated the membrane deflection  $d$  in its center versus applied external pressure  $\Delta P$ . It was found that  $\Delta P = Ad + Bd^3$  where  $A = 2.03 \text{ bar}/\mu\text{m}$  and  $B = 0.27 \text{ bar}/\mu\text{m}^3$ . This relation can be used to estimate the pressure in the chamber if  $d$  is known.

Figure 1: Design of the chip.



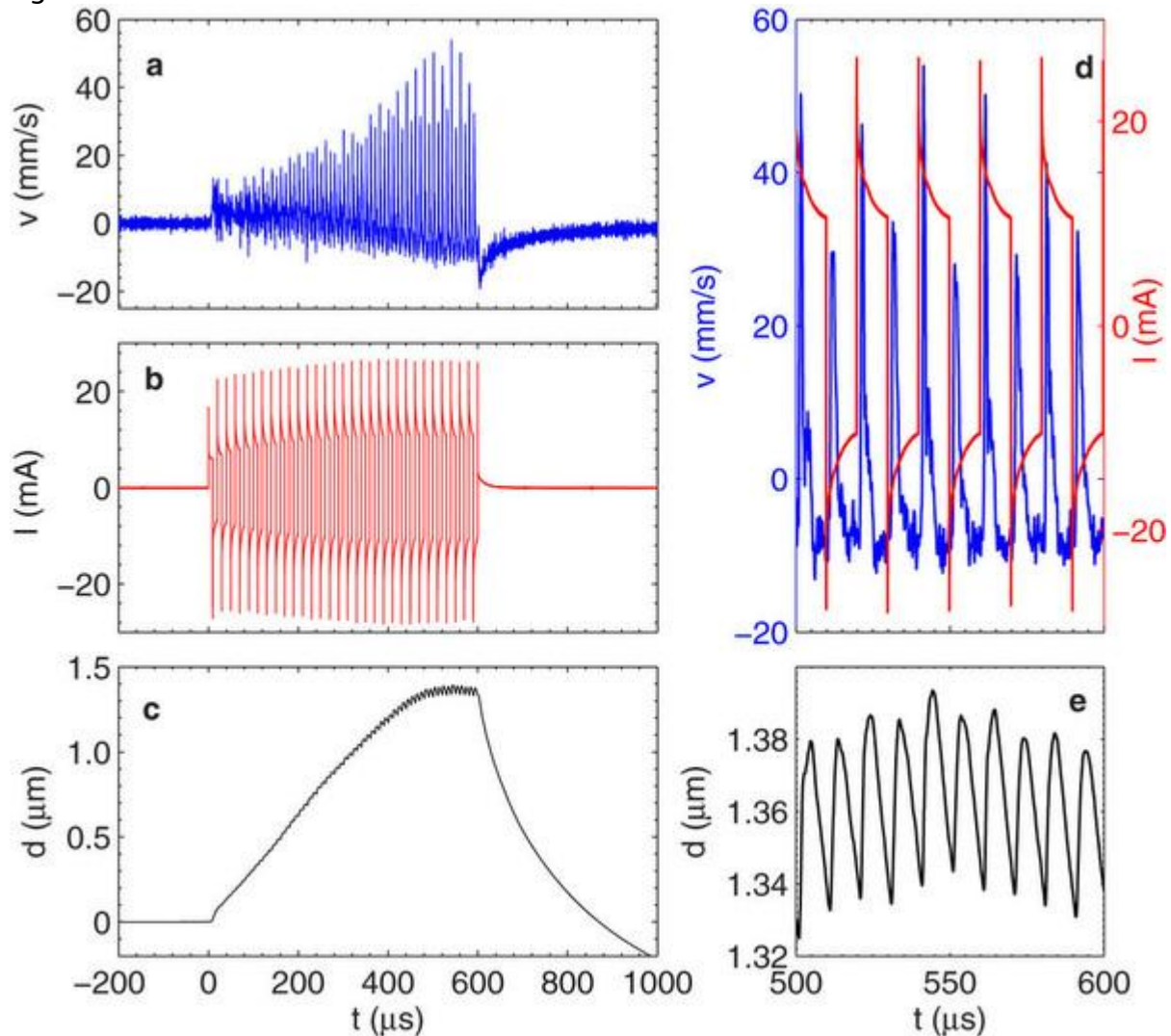
(a), A silicon wafer with a SiRN layer on top is bonded with a structured glass wafer. (b), Optical image of the chamber in the device before filling. The membrane (highlighted with green light from the bottom) is not completely etched, but normally it coincides with the size of the chamber. Under the central electrodes a thermal sensor (polysilicon) is visible. (c), General design of the chip: in/outlets, long channels, and six contact pads (2 for the electrodes and 4 for the sensor). (d), Completely functioning device glued to a PCB, sealed and wire bonded.

Short square voltage pulses were applied to the electrodes. The response of the system was observed with a homemade stroboscope<sup>25</sup> and with a vibrometer (Polytec MSA-400). In the latter case it was possible to observe the process from the top (via glass) or from the bottom focusing the laser beam ( $\lambda = 633 \text{ nm}$ ) with a diameter of  $1.5 \text{ }\mu\text{m}$  on the membrane. First, we measured the membrane deflection due to applied voltage pulses from the back side. For this configuration the change of the refractive index of the liquid due to different reasons (dissolved gas, heating, pressure change) does not influence the signal of the interferometer. Bubbles with the radius  $r > \lambda/2\pi$  appearing in the chamber can scatter the light because the membrane is transparent. To eliminate their effect on the signal we focused the laser beam on the opaque electrode. With these precautions we can be sure that the measured signal corresponds to the velocity of the membrane about  $10 \text{ }\mu\text{m}$  off its center

## Membrane deflection

For AP voltage pulses with the amplitude  $U = \pm 10$  V repeated with the frequency  $f = 50$  kHz (driving or switching frequency) during  $\tau = 600$   $\mu$ s the signal and current are shown in Fig. 2. The signal consists of separate narrow lines of increasing amplitude correlated with the driving pulses. It is well visible in Fig. 2d where only five periods for both the signal and current are shown in the same plot. The signal in Fig. 2a integrated over time  $t$  is the deflection of the membrane  $d(t)$ . It is shown in Fig. 2c. The deflection increases with time finally reaching a steady state while oscillations with the driving frequency  $f$  are superimposed on the smooth curve (see enlarged view in Fig. 2e). In its maximum the deflection becomes as high as  $d \approx 1.4$   $\mu$ m that corresponds to the pressure increase in the chamber  $\Delta P \approx 3.6$  bar.

Figure 2: Deflection of the actuator membrane measured from the back side.



The membrane is driven by AP voltage pulses  $U = \pm 10$  V,  $f = 50$  kHz, and  $\tau = 600$   $\mu$ s. (a), Velocity of the membrane (raw signal of the vibrometer). (b), Current flowing through the electrodes. (c), Deflection of the membrane (raw signal integrated over time). (d), Five last periods of the signal in (a) and the current in (b) are shown in the same plot. (e), Five last periods in the membrane deflection.

Our interpretation of the physical events presented in [Fig. 2](#) is the following. Stoichiometric nanobubbles that are formed nearby the electrode surface in phase with the electrical pulses<sup>6</sup> are responsible for the sharp peaks in [Fig. 2a and 2d](#). Previously we observed periodic reduction of gas concentration in the electrolyte above the electrodes<sup>6</sup>. Here we can see that in the closed chamber the process is accompanied also by the periodic variation of the pressure. This is an independent argument that the combustion reaction happens in the nanobubbles. The monotonic pressure increase in [Fig. 2c](#) is due to the gas existing as separate hydrogen and oxygen nanobubbles and dissolved molecules. The nanobubbles are formed homogeneously and very fast because the local supersaturations is high. For each period more gas is produced than consumed while a steady state is not reached. In the steady state a part of the produced gas disappears in correlation with the driving pulses (high frequency oscillation). The rest of gas gets into the reaction independently on the electrical pulses (randomly) by formation of stoichiometric nanobubbles in the solution. This random process is responsible for the fast decrease of the pressure after the switch off. The details of this interpretation can change, but the solid fact – the fast pressure decrease – has to be related to the reaction between H<sub>2</sub> and O<sub>2</sub>.

Source: <http://revolution-green.com/new-type-microengine-using-hydrogen-oxygen/>